Fourier Methods for Harmonic Scalar Waves in General Waveguides

Anders Andersson, Börje Nilsson, Thomas Biro

March 28, 2013

1 Introduction

Wave scattering in waveguides of different shapes is a classical problem in applied mathematics. The problem appears in many applications, in acoustics, optics, electro-dynamics and quantum physics.

When treating this problem mathematically, the task is to find solutions to the wave equation in some of its forms, and an essential part of this task is to solve Helmholtz equation

$$(\nabla^2 + k^2)p = 0 \tag{1}$$

in different geometries and with various boundary conditions.

For simple geometries, for example straight channels with hard or soft walls, the solutions are easily found in terms of Fourier series. Examples using this technique are found in any basic text on partial differential equations. For more complex geometries or boundary conditions, purely numerical methods or more precisely, finite element methods, have during recent years, due to evolution of both the methods and the computers, become the natural choice for solving Helmholtz equation.

However, motivated by both the mathematics and applications involving inverse wave scattering problems, we find it interesting to see what can be done with the classical semi-analytic Fourier methods, even when the geometries and the boundary conditions are complex.

The purpose of this article is exactly this, to investigate and to show how Fourier methods can be used to solve wave scattering problems in a waveguide with geometry and boundary conditions that exceed the ordinary school book examples. To be able to do that, we use a toolbox containing a set of methods:

- The Building Block Method makes it possible to divide a complicated geometry into several tractable parts.
- Different conformal mapping methods are used to further simplify the geometry.

- Reformulation of (1) assuming that the field can be expressed in Fourier series.
- Determination of numerically stable differential equations for reflection and transmission operators means that these can be determined for each part of the waveguide.
- Dirichlet-to-Neumann operators make it possible to formulate and solve numerically stable differential equations for the field in the waveguide.

Additional well-known tools such as mode matching and Wiener–Hopf methods, are necessary to solve general waveguide problems, but are not used in this article.

In an example taken from acoustic, i.e., the field in the waveguide is scalar, we show how these techniques can be combined, in order to get the complete solution of Helmholtz equation in a general waveguide. The results in this example are then compared with the results when using commercial finite element software to solve the problem.

The plan of the paper is as follows: In Section 2, the mathematical basis for a Fourier solution is outlined and in Section 3, it is described how the field as well as reflection and transmission operators are determined in a single "block", using conformal mappings and different reformulations of equation (1). Section 4 shows how these blocks can be combined, using the Building Block Method. Section 5 contains the example problem and a detailed description of the techniques used to solve it. Finally, some final comments are included in Section 6.

2 Preliminaries

The problem under investigation is propagation of scalar harmonic waves in a waveguide V, in $\mathbb{R}^2$ or $\mathbb{R}^3$, of rather general shape. Acoustic notation is used where the sound pressure p solves Helmholtz equation

$$(\nabla^2 + k^2)p(\boldsymbol{r}) = 0,\ \boldsymbol{r} \in V, \tag{2}$$

in the interior V of the waveguide and fulfils a homogeneous boundary condition

$$\frac{\partial p}{\partial n} = \mathrm{i}k\beta p,\ \boldsymbol{r} \in \partial V, \tag{3}$$

on the boundary ∂V. Here, $k \in \mathbb{R}^+$ is the wavenumber, $\beta \in \mathbb{C}$, $\operatorname{Re}\beta \geq 0$ is the (normalised) surface admittance and $\widehat{\boldsymbol{n}}$ is the outward pointing normal to ∂V. Special cases of the boundary conditions are $\beta = 0$ (Neumann or hard) and $\beta = \mathrm{i}\infty$ (Dirichlet or soft). The formulation assumes the time dependence $\exp(-\mathrm{i}kc_0t)$ in the underlying wave equation. In addition to the

sound velocity c_0, the acoustic medium in the waveguide is characterised by the density ρ_0. Both c_0 and ρ_0 are constant and real.

The waveguide $V \subset \mathbb{R}^n, n = 2, 3$, consists of three parts: an inner bounded and connected part V_i and two straight semi-infinite parts V_L and V_R. An axial co-ordinate u is associated to the waveguide with the positive axis aligned with V_R and the negative with V_L. Fig. 1 depicts this waveguide schematically. Using the notation $\mathbb{R}^{\pm}_{u_0} = \{u \in \mathbb{R} : \ u \gtrless u_0\}$, the

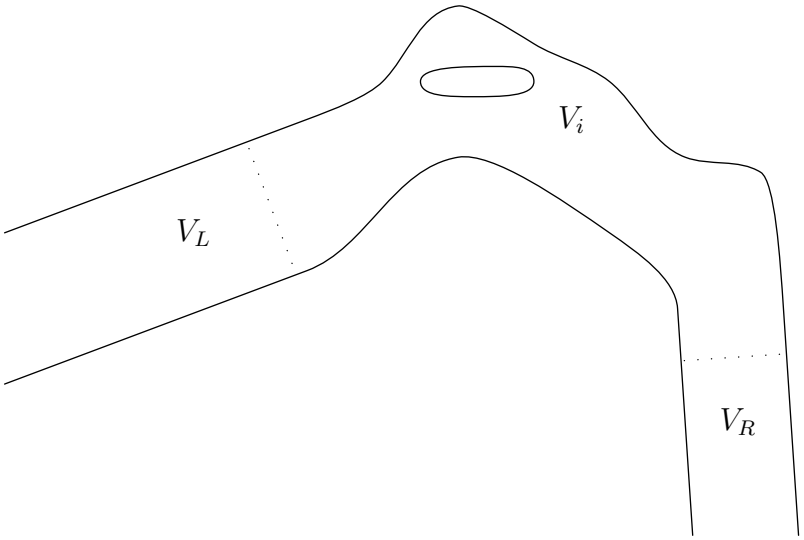

Figure 1: Waveguide $V = V_L \cup V_i \cup V_R$ consisting of straight parts V_L and V_R open to infinity and a bounded connecting part V_i.

straight waveguide parts are $V_\mathrm{L} = \Omega_\mathrm{L} \times \mathbb{R}^-_{u_\mathrm{L}}$ and $V_\mathrm{R} = \Omega_\mathrm{R} \times \mathbb{R}^+_{u_\mathrm{R}}$, where Ω_L and Ω_R are simply connected with boundary that is piecewise of class C^1. This means that Green's theorem is applicable. For simplicity it is assumed that the surface admittance $\beta = 0$ on $\partial V_\mathrm{L} \cap \partial V$ and on $\partial V_\mathrm{R} \cap \partial V$, whereas β can be non-vanishing and varying on V_i.

As a preparation for the definition of the scattering problem, we discuss propagation of waves in an infinite straight waveguide $V_\mathrm{s} = \Omega \times \mathbb{R}$, where Ω is Ω_L or Ω_R . If p solves (2) in V_s, p can be uniquely splitted into

$$p = p_- + p_+, \tag{4}$$

where

$$p_\pm = \sum_n p_n^\pm \mathrm{e}^{\pm \mathrm{i}\alpha_n u} \varphi_n(\boldsymbol{r}_\perp), \ \boldsymbol{r}_\perp \in \Omega. \tag{5}$$

Here, φ_n and $\lambda_n \geq 0$ are solutions to the eigenvalue problem

$$\begin{cases} (\nabla_\perp^2 + \lambda_n^2)\varphi_n(\boldsymbol{r}_\perp) = 0, \ \boldsymbol{r}_\perp \in \Omega \\ \dfrac{\partial \varphi_n}{\partial n}(\boldsymbol{r}_\perp) = 0, \ \boldsymbol{r}_\perp \in \partial\Omega \\ \int_\Omega \varphi_n^2(\mathbf{r}_\perp)\mathrm{d}\Omega = 1 \end{cases}, \tag{6}$$

$\nabla_\perp^2$ is the restriction of the Laplace operator to Ω, and

$$\alpha_n = \begin{cases} \sqrt{k^2 - \lambda_n^2}, \ k \geq \lambda_n \\ \mathrm{i}\sqrt{\lambda_n^2 - k^2}, \ k < \lambda_n \end{cases}. \tag{7}$$

We are interested in a solution p that has a finite (real and virtual) acoustic power in the axial direction and define to this end the function space

$$X_\pm = \left\{ p_\pm = \textstyle\sum_n p_n^\pm \mathrm{e}^{\pm \mathrm{i}\alpha_n u}\varphi_n(\boldsymbol{r}_\perp) : \sum_n |\alpha_n| \left|p_n^\pm\right|^2 < \infty \right\} \tag{8}$$

and $X = X_- \oplus X_+$. Then, $p_- \in X_-$, $p_+ \in X_+$ and $p \in X$.

If $p_+ \neq 0$, we say that there is a source at $u = -\infty$, and if $p_- \neq 0$, there is a source at $u = +\infty$. Assume that there is a region $V_0 \subset V$, containing sources, i.e., where $(\nabla^2 + k^2)p \neq 0$, and that this source region is confined to the interval $u_- < u < u_+$. In physical terms, there should be only outgoing waves outside the source region, i.e., leftgoing to the left and rightgoing to the right. In order to couple this requirement to our definition of p_- and p_+, we formulate the following

Axiom 1.

For the solution to $(\nabla^2 + k^2)p = -q$ *in* V_s, *where* $q = 0$ *for* $u < u_-$ *and* $u > u_+$,

$$\begin{array}{l} p = p_-, \ \textit{when } u < u_- \textit{ and there is no source in } u = -\infty \\ p = p_+, \ \textit{when } u > u_+ \textit{ and there is no source in } u = +\infty \end{array}.$$

Comment 1 Axiom 1 makes it natural to denote p_- as leftgoing and p_+ as rightgoing.

Comment 2 Axiom 1 can be derived from physical principles: (a) According to the principle of vanishing absorption, k is replaced by $k + \mathrm{i}\varepsilon$, $\varepsilon > 0$, requiring that the solution p tends to zero when the distance to the source region tends to infinity; then the limit of vanishing ε is taken. (b) According to the principle of causality, which is a fundamental physical principle, asymptotic or stationary solutions for large t to the wave equation $(\nabla^2 - c_0^{-2}\partial^2/\partial t^2)p = -q(\boldsymbol{r})\mathrm{H}(t)\sin(kc_0 t)$ is studied, where $\mathrm{H}(t)$ is Heaviside's step function. For both cases a) and b), Axiom 1 follows with $p_\pm$ according to (5-7).

3 Solving the one-block problems

Wave scattering in a complicated geometry with varying boundary conditions can be treated as a series of simpler problem, using the so called Building Block Method, see Section 4. The method determines reflection and transmission operators for the waveguide, given that these operators have been determined for each section ("block") of the waveguide.

In this section, we show how reflection and transmission operators for a single block are established, but also, using a Dirichlet-to-Neumann formulation, how the acoustic wave field inside the block could be determined. When performing these calculations, interactions from the two ends of the block must be avoided, and hence, each block is assumed to be an infinitely long waveguide with parallel straight walls and constant boundary conditions outside some bounded transition region.

In each such geometry, the boundary value problem

$$\begin{cases} \left(\nabla^2 + k^2\right) p(x,y) = 0 & \text{in the waveguide,} \\ \dfrac{\partial p}{\partial n} = \mathrm{i}k\beta(t)p & \text{on the boundary,} \end{cases} \tag{9}$$

where β varies smoothly with some boundary parameter t, should be solved. For the sake of simplicity, we assume that one of the channel walls is hard, giving a Neumann boundary condition there.

We use a conformal mapping

$$F : w = u + \mathrm{i}v \to z = x + \mathrm{i}y$$

to transform the geometry into a straight horizontal channel $\{u \in \mathbb{R}, 0 \leq v \leq 1\}$ in the (u,v)-plane, see Fig. 2. After this transformation, Eq. (9) yields

$$\begin{cases} \left(\nabla^2 + k^2\mu(u,v)\right) \Phi(u,v) = 0 \\ \left.\dfrac{\partial \Phi(u,v)}{\partial v}\right|_{v=1} = \mathrm{i}kY(u)\Phi(u,1) \\ \left.\dfrac{\partial \Phi(u,v)}{\partial v}\right|_{v=0} = 0 \end{cases} \tag{10}$$

where $\mu(u,v) = |F'(w)|^2$ and $Y(u) = \beta(u)\,|F'(u+i)|$.

Following the techniques, outlined in [3], where an electro-magnetic scattering problem is treated, or [15], where similar problems from acoustics are solved, we expand $\Phi(u,v)$ in cosine Fourier series over v, assuming that

$$\Phi(u,v) = \sum_n \Phi_n(u)\varphi_n(u,v), \tag{11}$$

where $\varphi_n(u,v) = \cos(v\lambda_n(u))$ for functions $\lambda_n(u), \quad n \in \mathbb{N}$.

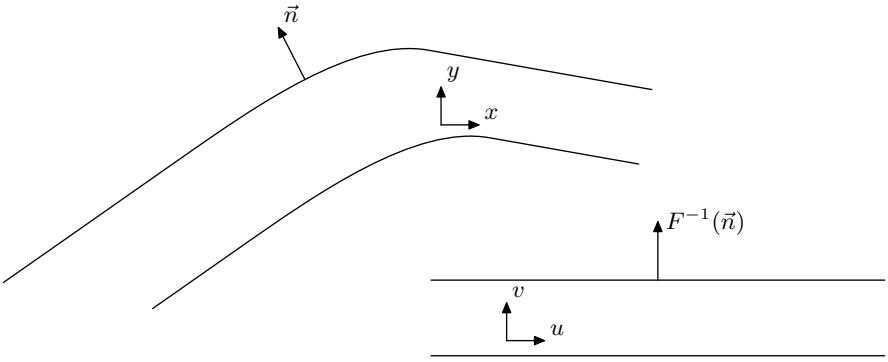

Figure 2: A single block in the $z = x + \mathrm{i}y$ plane and the $w = u + \mathrm{i}v$ plane.

The functions λ_n are determined by the boundary condition (10), from which follows that $\lambda_n(u)$, $n = 0, 1, \ldots$, are solutions to the equation

$$\lambda_n(u)\tan\big(\lambda_n(u)\big) = -\,\mathrm{i}kY(u). \tag{12}$$

By differentiating (12), it follows that

$$\lambda_n'(u) = \frac{-\,\mathrm{i}kY'(u)}{Q(u)} \tag{13}$$

and

$$\lambda_n''(u) = -\,\mathrm{i}k\left(\frac{Y''(u)Q(u) - Y'(u)Q'(u)}{\big(Q(u)\big)^2}\right) \tag{14}$$

where $(')$ stands for differentiating with respect to u and

$$Q(u) = \tan\big(\lambda(u)\big) + \lambda(u)\Big(1 + \tan^2\big(\lambda(u)\big)\Big).$$

From the expansions

$$v\sin(v\lambda_n(u)) = \sum_m \alpha_{mn}(u)\cos(v\lambda_m(u)), \tag{15}$$

$$v^2\cos(v\lambda_n(u)) = \sum_m \beta_{mn}(u)\cos(v\lambda_m(u)), \tag{16}$$

$$\mu(u,v)\cos(v\lambda_n(u)) = \sum_m \mu_{mn}(u)\cos(v\lambda_m(u)), \tag{17}$$

follows the infinite-dimensional ordinary differential equation

$$\boldsymbol{\Phi}''(u) - A(u)\boldsymbol{\Phi}'(u) - B^2(u)\boldsymbol{\Phi}(u) = 0, \tag{18}$$

where the infinite vector $\boldsymbol{\Phi} = (\Phi_1\Phi_2\Phi_3\ldots)^T$ and the infinite matrices A and B^2 have elements

$$A_{mn}(u) = 2\alpha_{mn}(u)\lambda_n'(u) \tag{19}$$

and

$$B_{mn}^2(u) = \alpha_{mn}(u)\lambda_n''(u) + \beta_{mn}(u)\left(\lambda_n'(u)\right)^2 + \delta_{mn}\left(\lambda_n(u)\right)^2 - k^2\mu_{mn}(u). \quad (20)$$

Note that (φ_m), with $\varphi_m(v) = \cos v\lambda_m(u)$, is in general not an orthogonal system since the eigenvalue problem (10) is a regular Sturm-Liouville problem only if Y is purely imaginary. However, (φ_m) and $(\overline{\varphi_m})$, with a bar $\bar{\cdot}$ denoting the complex conjugate, form a biorthogonal system meaning that the bilinear form

$$\langle \varphi_m, \varphi_n \rangle = (\varphi_m, \overline{\varphi_n}) = \int_0^1 \varphi_m(v)\varphi_n(v)\mathrm{d}v, \quad (21)$$

vanishes if $n \neq m$. Here, for complex functions f and g, (f, g) denotes the complex scalar product and the bilinear form $\langle f, g \rangle$ is formally the same as the real scalar product. This means that the expansion coefficients like $\alpha_{mn}(u), \beta_{mn}(u)$ and $\mu_{mn}(u)$ in (15–17), are found from

$$a_m = \frac{\langle f, \varphi_m \rangle}{\langle \varphi_m, \varphi_m \rangle} \quad (22)$$

for the expansion

$$f = \sum_m a_m \varphi_m. \quad (23)$$

Furthermore, the system (φ_m) is proved to be complete in $L^2(0, 1)$ using Hilbert space techniques [4],[5] but Paley-Wiener space techniques [16] could also be used; see also [12] for a general treatise on eigenvalue problems based on functional analysis for differential equations with two-point boundary conditions such that like (10), the related operator is non-self-adjoint. It is also worth noting [7] that the completeness property for (φ_m) can be analysed as an analytic continuation of (22) from purely imaginary Y, for which completeness holds, to general Y.

3.1 Conformal mapping techniques

There are two indispensable requirements on the conformal mapping. When determining reflection and transmission operators for a single waveguide block, as well as the field inside the block, we must assume no interactions from the ends of the block. This is accomplished by treating the block as an infinite waveguide which is straight and has constant cross-sections outside some bounded region. We must therefore numerically construct a conformal mapping from a straight infinite channel to an infinite channel in which the walls at both ends are (at least) asymptotically straight and parallel. Furthermore, to avoid singularities in the operators A and B^2 in the differential equation (18), it follows from (10) that the mapping must have a bounded first derivative on the boundary, and additionally, from (13),

(14), (19) and (20), bounded second and third derivatives if the boundary has non-zero admittance.

In [1] and [2], conformal mapping techniques, suitable for this situation, are developed. Both methods are built on the Schwarz–Christoffel mapping, which guarantees that the resulting channel walls are asymptotically straight and parallel towards infinity, and they both result in regions with smooth boundary curves, meaning that no singularities are introduced by the mapping. In [1], a suitable polygon, surrounding the region under consideration, is determined, and the conformal mapping is constructed by using the Schwarz–Christoffel mapping for that polygon. In [2], the factors in a Schwarz–Christoffel mapping are replaced by so called approximate curve factors that round the corners in a way that gives a smooth boundary curve.

3.2 Accomplishing stable equations

The differential equation (18) cannot be solved directly by numerical methods. However, there exist reformulations of (18) that are numerically stable for all but a countable set of k, i.e. for $k \notin \{k_1, k_2, k_3, \dots\}$. In this section, we describe two such reformulations, built on two different partitions of the wave field $\boldsymbol{\Phi}$.

Recall that the block is assumed to be an infinitely long waveguide which is straight and has parallel hard boundaries outside some central transition region. Let Ω_L and Ω_R be the straight regions to the left and right respectively. In Ω_L and Ω_R, the operator A is zero, while B is constant. Assume that $B = B_-$ in Ω_L and $B = B_+$ in Ω_R. In Ω_L and Ω_R, B^2 is a real constant diagonal matrix, and to be consistent with standard theory for straight waveguides, the square roots of B^2 are chosen such that B_- and B_+ have either positive real or negative imaginary diagonal elements.

3.2.1 Determining Reflection and Transmission operators (The RT method)

Inspired by the partition $p = p_- + p_+$ in a straight waveguide where the two terms can be seen as representing waves marching from left to right and right to left respectively, we make the following definition: Let for all $u \in \mathbb{R}$, the wave field

$$\boldsymbol{\Phi}(u) = (\Phi_1(u)\ \Phi_2(u)\ \dots)^T = \boldsymbol{\Phi}^+(u) + \boldsymbol{\Phi}^-(u), \tag{24}$$

where $\boldsymbol{\Phi}^+(u)$ and $\boldsymbol{\Phi}^-(u)$ represent waves marching to the right and left respectively.

Let furthermore C and D be operators, depending on u, such that

$$\frac{\partial \boldsymbol{\Phi}}{\partial u}(u) = -C(u)\boldsymbol{\Phi}^+(u) + D(u)\boldsymbol{\Phi}^-(u), \tag{25}$$

for all $u \in \mathbb{R}$. C and D can be defined in many different ways, but they must be differentiable with respect to u, and since (18) must hold in Ω_L and Ω_R where $A(u) = 0$, it follows that $C = D = B_-$ in Ω_L and $C = D = B_+$ in Ω_R. We have used the definition

$$C(u) = D(u) = B_- + f(u)(B_+ - B_-), \tag{26}$$

where f is a smooth function that is 0 in Ω_L and 1 in Ω_R.

Define reflection and transmission operators R^+, R^-, T^+, T^-, such that for $u_1 < u_2$,

$$\begin{pmatrix} \boldsymbol{\Phi}^+(u_2) \\ \boldsymbol{\Phi}^-(u_1) \end{pmatrix} = \begin{pmatrix} T^+(u_2, u_1) & R^-(u_1, u_2) \\ R^+(u_2, u_1) & T^-(u_1, u_2) \end{pmatrix} \begin{pmatrix} \boldsymbol{\Phi}^+(u_1) \\ \boldsymbol{\Phi}^-(u_2) \end{pmatrix}. \tag{27}$$

This means that T^- and R^- transmits respectively reflects the left-going waves $\boldsymbol{\Phi}^-$, while T^+ and R^+ transmits respectively reflects the right-going waves $\boldsymbol{\Phi}^+$.

From (18), (24) and (25), it is possible to derive, for details see for example [15], the equation

$$\frac{\partial}{\partial u} \begin{pmatrix} \boldsymbol{\Phi}^+ \\ \boldsymbol{\Phi}^- \end{pmatrix} = \begin{pmatrix} J & K \\ L & M \end{pmatrix} \begin{pmatrix} \boldsymbol{\Phi}^+ \\ \boldsymbol{\Phi}^- \end{pmatrix}, \tag{28}$$

where

$$\begin{aligned} J &= (C + D)^{-1} \left(-C' - B^2 + (A - D)C \right), \\ K &= (C + D)^{-1} \left(D' - B^2 - (A - D)D \right), \\ L &= (C + D)^{-1} \left(C' + B^2 - (A + C)C \right), \\ M &= (C + D)^{-1} \left(-D' + B^2 + (A + C)D \right). \end{aligned} \tag{29}$$

For the determination of T^+ and R^+, we consider (27) assuming that there are no sources in Ω_R. Let $u_2 \in \Omega_R$ be constant and let $u = u_1$ vary. This means that $\boldsymbol{\Phi}^-(u_2) = 0$, and (27) simplifies to

$$\begin{cases} T^+(u_2, u)\boldsymbol{\Phi}^+(u) = \boldsymbol{\Phi}^+(u_2), \\ R^+(u_2, u)\boldsymbol{\Phi}^+(u) = \boldsymbol{\Phi}^-(u). \end{cases} \tag{30}$$

By differentiating (30) with respect to u, we get

$$\begin{cases} \dfrac{\partial T^+}{\partial u}(u_2, u)\boldsymbol{\Phi}^+(u) + T^+(u_2, u)\dfrac{\partial \boldsymbol{\Phi}^+}{\partial u}(u) = 0, \\ \dfrac{\partial R^+}{\partial u}(u_2, u)\boldsymbol{\Phi}^+(u) + R^+(u_2, u)\dfrac{\partial \boldsymbol{\Phi}^+}{\partial u}(u) = \dfrac{\partial \boldsymbol{\Phi}^-}{\partial u}(u), \end{cases} \tag{31}$$

and using (28) and (30) once more, the Ricatti equations

$$\begin{aligned}\frac{\partial R^+}{\partial u}(u_2,u) = -R^+(u_2,u)\big(J(u)+K(u)R^+(u_2,u)\big)\\ + L(u) + M(u)R^+(u_2,u)\end{aligned} \tag{32}$$

$$\frac{\partial T^+}{\partial u}(u_2,u) = -T^+(u_2,u)\big(J(u)+K(u)R^+(u_2,u)\big) \tag{33}$$

follow. For R^- and T^-, we proceed similarly assuming no sources in Ω_L, and deduce the equations

$$\begin{aligned}\frac{\partial R^-}{\partial u}(u,u_1) = -R^-(u,u_1)\big(M(u)+L(u)R^-(u,u_1)\big)\\ + K(u) + J(u)R^-(u,u_1),\end{aligned} \tag{34}$$

$$\frac{\partial T^-}{\partial u}(u,u_1) = -T^-(u,u_1)\big(M(u)+L(u)R^-(u,u_1)\big). \tag{35}$$

Using truncated matrices in place of J, K, L and M, these equations can be solved numerically with an ordinary differential equation solver. (32) and (33) are solved from right to left using $R^+(u_2,u_2)=0$ and $T^+(u_2,u_2)=I$ as initial values, while (34) and (35) are solved from left to right, using $R^-(u_1,u_1)=0$ and $T^-(u_1,u_1)=I$ as initial values.

3.2.2 Determining the field (The DtN method)

To determine the field inside a single block, we reformulate (18) using Dirichlet-to-Neumann operators, see also [13] and [6]. For this purpose, we make a different partition of $\boldsymbol{\Phi}$. Let

$$\boldsymbol{\Phi} = \boldsymbol{\Phi}_R + \boldsymbol{\Phi}_L, \tag{36}$$

where $\boldsymbol{\Phi}_R$ are waves with no sources to the right (in $+\infty$) and $\boldsymbol{\Phi}_L$ are waves with no sources to the left (in $-\infty$). Define Dirichlet to Neumann (DtN) operators Λ_R and Λ_L such that

$$\boldsymbol{\Phi}_R'(u) = -\Lambda_R(u)\boldsymbol{\Phi}_R(u), \tag{37}$$

$$\boldsymbol{\Phi}_L'(u) = \Lambda_L(u)\boldsymbol{\Phi}_L(u). \tag{38}$$

Φ_R and Φ_L are both satisfying (18), and by differentiating (37) and (38), the operator equations

$$\Lambda_R'(u) = \big(A(u)+\Lambda_R(u)\big)\Lambda_R(u) - B^2(u) \tag{39}$$

$$\Lambda_L'(u) = \big(A(u)-\Lambda_L(u)\big)\Lambda_L(u) + B^2(u) \tag{40}$$

follow. Since $A=0$ in Ω_L and Ω_R,

$$\boldsymbol{\Phi}_R'(u) + B_-\boldsymbol{\Phi}_R(u) = 0, \quad \boldsymbol{\Phi}_L'(u) - B_-\boldsymbol{\Phi}_L(u) = 0, \qquad u\in\Omega_L, \tag{41}$$

$$\boldsymbol{\Phi}_R'(u) - B_+\boldsymbol{\Phi}_R(u) = 0, \quad \boldsymbol{\Phi}_L'(u) + B_-\boldsymbol{\Phi}_L(u) = 0, \qquad u\in\Omega_R, \tag{42}$$

which means that if truncated matrices are used in place of A and B^2, (39) and (40) can be solved numerically from right and left respectively, using the initial values $\Lambda_R(u_2) = B_+$ and $\Lambda_L(u_1) = B_-$, where $u_1 \in \Omega_L$ and $u_2 \in \Omega_R$. Finally, (37) and (38) are solved numerically from left and right respectively.

It is worth noticing that the Riccati equations (32-35) as well as (39-40) can for a countable set of k contain singularities for certain values of u and resist a numerical solution, for details and examples see for example [6]. However, these singularities appears for k values in the DtN equations (39-40) for which the RT equations (32-35) have no problem, so the different methods complete each other well. Furthermore, there exist numerical methods by which Riccati matrix equations are integrated across singularities, even when no knowledge about existence or placements of these is at hand, see for example [11].

4 Combining the Blocks - the Building Block Method

The Building Block Method (BBM), see [14], allows the determination of reflection and transmission operators for a combination of several sections ("blocks") of the waveguide, for which these operators are known.

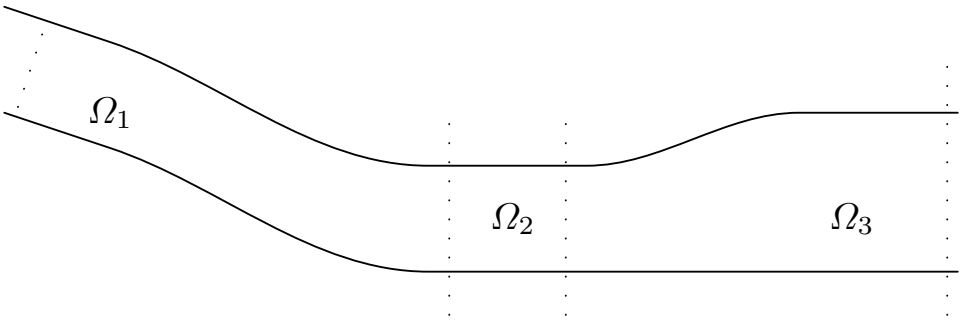

Figure 3: Waveguide divided in blocks. Ω_2 is straight and with constant cross-section.

Assume that two subsequent blocks Ω_1 and Ω_3, are connected by a region Ω_2 which is straight and with constant cross-section, see figure 3. For simplicity, we assume that Ω_2 is parallel to the x-axis. Furthermore, assume that reflection and transmission operators in matrix form for Ω_1 and Ω_2 are known.

In contrast to many descriptions of the BBM, we choose here to define $\boldsymbol{\Phi} = \boldsymbol{\Phi}^+ + \boldsymbol{\Phi}^-$ as varying with the position along the waveguide, even outside and between the blocks. The reflection and transmission operators are defined accordingly: Assume that a block begins and ends at position a and b respectively and that there are no sources at the b side of the block. If $T^+ (= T^+(b, a))$ is the transmission operator for waves $\boldsymbol{\Phi}^+$ entering the block

at a, then $\boldsymbol{\Phi}^+(b) = T^+\boldsymbol{\Phi}^+(a)$ are the waves leaving the block at position b. Let t be a parameter, measuring the distance along the central curve of the waveguide, and let $t = t_0$ at the beginning (left end) of Ω_1, $t = t_1 = 0$ at the border between Ω_1 and Ω_2, $t = t_2 = \ell$ at the border between Ω_2 and Ω_3, assuming that the length of Ω_2 is ℓ, and finally $t = t_3$ at the end of Ω_3. Furthermore, we use the following denotation:

Symbol	Explanation
R_1^+	Reflection operator for Ω_1 for waves entering from the left.
T_1^+	Transmission operator for Ω_1 for waves entering from the left.
R_1^-	Reflection operator for Ω_1 for waves entering from the right.
T_1^-	Transmission operator for Ω_1 for waves entering from the right.
R_3^+	Reflection operator for Ω_3 for waves entering from the left.
T_3^+	Transmission operator for Ω_3 for waves entering from the left.
R_{tot}^+	Reflection operator for $\cup_{j=1}^3 \Omega_j$ for waves entering from the left.
T_{tot}^+	Transmission operator for $\cup_{j=1}^3 \Omega_j$ for waves entering from the left.

For the straight part Ω_2 with length ℓ and width a, we define

$$S(t) = \begin{pmatrix} \mathrm{e}^{\mathrm{i}\alpha_0 t} & 0 & 0 & \cdots \\ 0 & \mathrm{e}^{\mathrm{i}\alpha_1 t} & 0 & \cdots \\ 0 & 0 & \mathrm{e}^{\mathrm{i}\alpha_2 t} & \\ \vdots & \vdots & & \ddots \end{pmatrix}, \quad 0 \le t \le \ell, \tag{43}$$

where $\alpha_n = \sqrt{k^2 - \dfrac{n^2\pi^2}{a^2}}$.

Assume that a right-marching field $\boldsymbol{\Phi}^{\text{in}} = \Phi^+(t_0)$ is entering Ω_1 from the left, and that there are no sources to the right of Ω_3. Define operators $C^\pm$ such that at the border between Ω_1 and Ω_2, $\Phi^+(0) = C^+(0)\boldsymbol{\Phi}^{\text{in}}$ and $\Phi^-(0) = C^-(0)\boldsymbol{\Phi}^{\text{in}}$. Standard theory for straight waveguides gives that in Ω_2 at position t, the field is

$$\boldsymbol{\Phi}(t) = (S(t)C^+ + S^{-1}(t)C^-)\boldsymbol{\Phi}^{\text{in}}. \tag{44}$$

Consequently, at the border between Ω_2 and Ω_3, there are right-marching and left-marching waves $S(\ell)C^+\boldsymbol{\Phi}^{\text{in}}$ and $S^{-1}(\ell)C^-\boldsymbol{\Phi}^{\text{in}}$ respectively.

Since there are no sources to the right of Ω_3, $S^{-1}(\ell)C^- = R_3^+S(\ell)C^+$, so $C^- = S(\ell)R_3^+S(\ell)C^+$. But $C^+ = T_1^+ + R_1^-C^-$, and hence

$$\begin{aligned} C^+ &= \left(I - R_1^-S(\ell)R_3^+S(\ell)\right)^{-1} T_1^+, \\ C^- &= S(\ell)R_3^+S(\ell)C^+, \\ T_{\text{tot}}^+ &= T_3^+S(\ell)C^+, \\ R_{\text{tot}}^+ &= R_1^+ + T_1^-C^-. \end{aligned} \tag{45}$$

The methods has been known since the end of the 1940:s [10] and is denoted the Building Block Method [14] in acoustic theory and cascade technique [9] in electromagnetic theory.

5 A numerical example

To illustrate the techniques, we solve the scattering problem and determine a low-frequency field in the waveguide shown in Fig. 4. The results, i.e., the

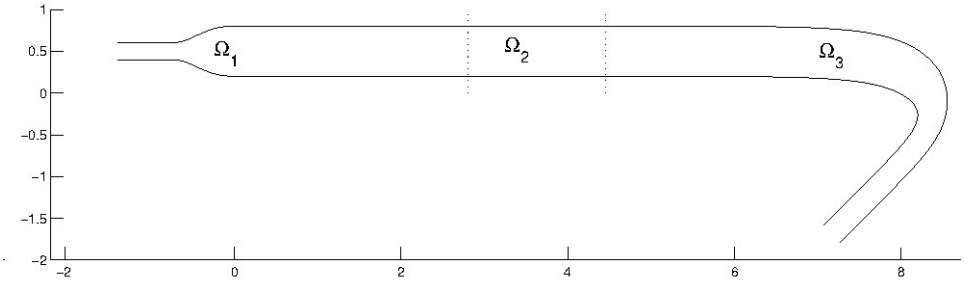

Figure 4: The waveguide in the example.

acoustic field in the waveguide given a known field entering from the left, as well as reflection as transmission operators for the waveguide, are calculated and compared with a finite element method solution.

5.1 Boundary conditions

The boundaries are hard, i.e., have zero admittance, except for two intervals on the upper boundary. In both Ω_1 and Ω_3, there is admittance at the upper boundary in the intervals $F_j([-2,2]+\mathrm{i})$ for $j \in \{1,2\}$, reaching the maximal level $\beta = 0.5 + 0.5\,\mathrm{i}$ in the intervals $F_j([-1,1]+\mathrm{i})$, where the functions F_j are the conformal mappings defined in Section 5.2.

5.2 Conformal mappings

The region is divided into three disjoint parts. Ω_1 contains the change in cross-section to the left, the middle section Ω_2 is straight with constant cross-section, and Ω_3 contains the bending to the right.

For Ω_1, shown in Fig. 5(a), a conformal mapping is constructed using the approximate curve factor technique developed in [2]. The conformal mapping is $F_1 = f_1 \circ g_1$, where

$$f_1(w) = A \int_{w_0}^{w} \prod_{j=1}^{4} \left(\sqrt{(\omega + b_k\,\mathrm{i} - w_k)^2 - c_k^2} - b_k\,\mathrm{i} \right)^{\alpha_k - 1} \omega^{-1} d\omega + z_0, \quad (46)$$

and

$$g_1(w) = \exp(\pi w). \tag{47}$$

In (46), $A = 0.6/\pi$ to get the width 0.6 to the right, $\boldsymbol{\alpha} = (0.85, 1.15, 1.15, 0.85)^t$ to get inner angles of sizes 1.15π and 0.85π, $\boldsymbol{b} = \boldsymbol{c} = (1, 0.05, 0.05, 1)^t$ to get the corners appropriately rounded, and $\boldsymbol{w} = (-1, -a, a, 1)^t$, where $a = 0.008740$ has been numerically determined to get the width 0.2 to the left. Finally, w_0 is set to 2 and z_0 to $1 + 0.2i$ to position the waveguide in the complex plane.

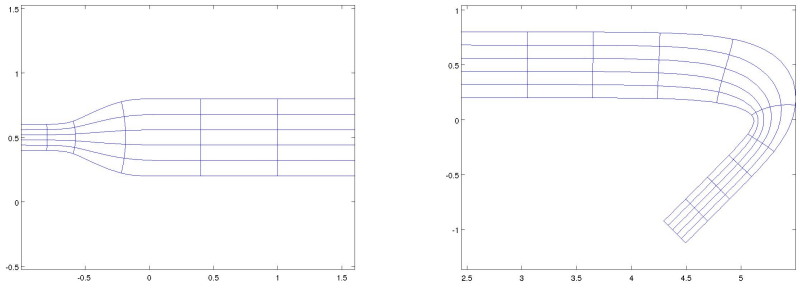

Figure 5: The two building blocks. The grid lines are images under the conformal mappings of $u = -5, -4, ..., 4, 5$ and $v = 0, 0.2, \ldots, 1$.

For Ω_3, shown in Fig. 5(b), the outer polygon method [1] is used to construct the conformal mapping. The mapping function is here $F_2 = f_2 \circ g_2$, where

$$f_2(w) = \int_{g_2(w_0)}^{w} \frac{(\omega - 1)^{\alpha - 1}}{(\omega + 1)^{\alpha - 1}(\omega - a)}\, d\omega + z_0 \tag{48}$$

and

$$g_2(w) = w^{(\varphi_2 - \varphi_1)/\pi}\, \mathrm{e}^{\,\mathrm{i}\varphi_1} + a, \tag{49}$$

with $A = 0.1501 \exp(3\pi\,\mathrm{i}/4)$, $\alpha = 7/4$, $\varphi_1 = 3\pi/10$, $\varphi_2 = 7\pi/10$, $a = -0.4632$, $w_0 = -7$ and $z_0 = 4.4485 + 0.2\,\mathrm{i}$.

5.3 Determination of the field, reflection and transmission operators

The acoustic fields inside Ω_1 and Ω_3 have been determined using the techniques described in Section 3.2.2. Simultaneously, reflection and transmission operators for Ω_1 and Ω_3 have been determined using the techniques in Section 3.2.1. All calculations have been made using 10×10 matrices in place of the operators in the differential equations (32)–(35) and (37–40) and a standard numerical ODE solver (`ode45`).

We have assumed a source at infinity to the left resulting in a right-marching wave $\boldsymbol{\Phi}_{\text{in}} = (1\ 0\ 0\ 0 \ldots)^t$ entering the waveguide from the left. No sources to the right is assumed.

The matrices $A(u)$ and $B^2(u)$ in (18), as well as the matrices J, K, L and M in (29) have been determined for $u = -5, -4.99, ..., 5$ in Ω_1, and for $u = -7, -6.99, ..., 7$ in Ω_3. Linear interpolation was then used in the ODE solvers to determine J, K, L and M in eqs. (32–35) and A and B^2 in eqs. (39) and (40) for u values not in this set.

Finally, the field in Ω_2 as well as reflection and transmission operators for the whole waveguide was calculated using the Building Block Method described in Section 4.

5.4 Results

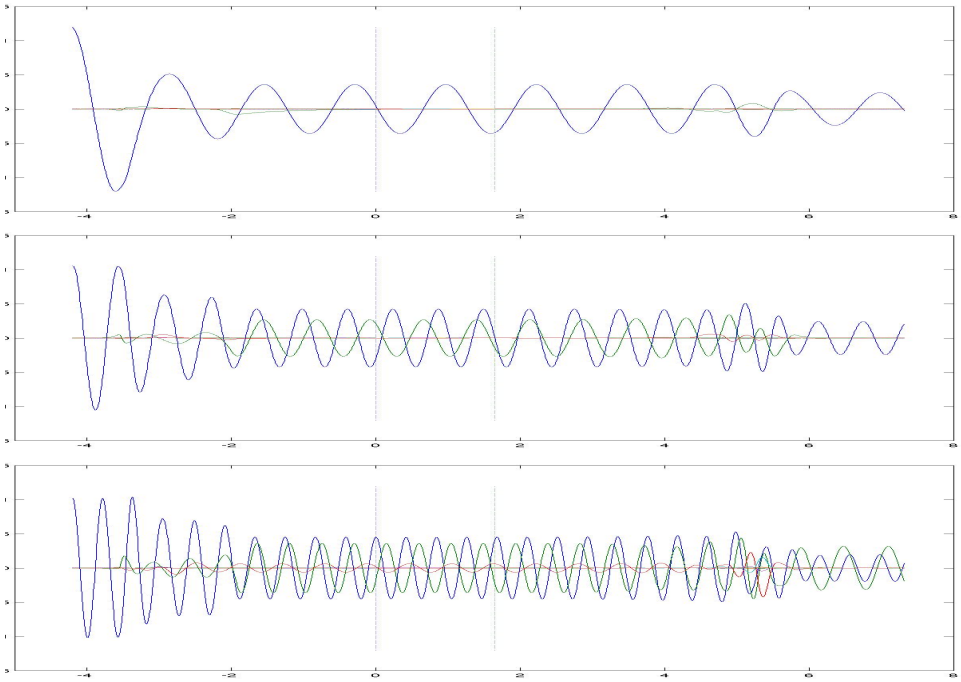

Figure 6: $\mathrm{Re}\,\Phi_1, \mathrm{Re}\,\Phi_2, \mathrm{Re}\,\Phi_3, \ldots$ for $k = 5$, $k = 10$ and $k = 15$. Dotted vertical lines indicate borders between Ω_1, Ω_2 and Ω_3.

In Figure 6, $\mathrm{Re}\,\Phi_1, \mathrm{Re}\,\Phi_2, \ldots$ is plotted for $k = 5$, $k = 10$ and $k = 15$. The measure on the horizontal axis in the plot is the distance along the central curve in the waveguide. In Figure 7, a contour plot of $\mathrm{Re}\,p(x, y)$ is shown for $k = 15$.

Note that in Ω_1, $\boldsymbol{\Phi}$ is calculated using the methods in Section 3.2.2, while in Ω_2, where it is calculated using (44) and (45), $\boldsymbol{\Phi}$ depends on the reflection and transmission operators found by the methods in Section 3.2.1. It is therefore interesting to compare $\boldsymbol{\Phi}$ in the right end of Ω_1 with $\boldsymbol{\Phi}$ in the left end of Ω_2, i.e. with $(C^+ + C^-)\boldsymbol{\Phi}^{\mathrm{in}}$. Likewise, it is interesting to compare

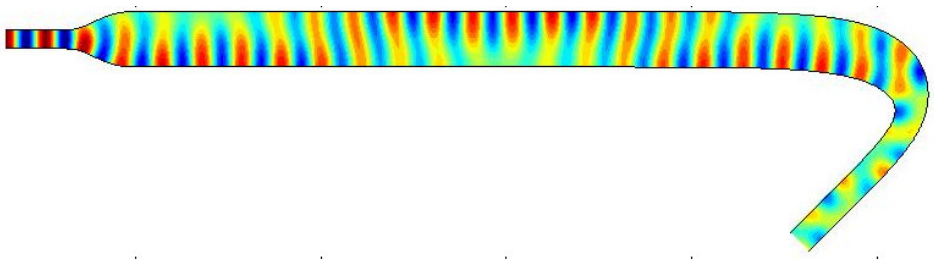

Figure 7: $\mathrm{Re}\, p(x, y)$ plotted for $k = 15$.

$\boldsymbol{\Phi}$ at the end of Ω_3, calculated with the DtN method, with $T^+_{\mathrm{tot}}\boldsymbol{\Phi}^{\mathrm{in}}$, where T^+_{tot} is determined using the RT method and the Building block method.

These comparisons are given in Table 1, and show that the correspondence between the methods is good.

5.5 A FEM solution to the problem

The Finite Element Method (FEM) is a well-established process for treating problems like the one in the example, and it is probably the most used method to solve such problems. As a comparison, we have applied a commercial FEM solver (COMSOL Multiphysics) to the problem. In Figure 8, FEM solutions for $k = 0..20$ are compared with the corresponding Fourier method solutions. As is seen in the figure, the correspondence is good. The differences between the methods in the calculated k interval are all less than $4 \cdot 10^{-3}$.

6 Discussion and conclusion

The example problem in Section 5 is of course not a "general" waveguide. There are numerous possible boundary variations not commented so far.

	$\boldsymbol{\Phi}_{\Omega_1}(\mathrm{end})$	$\boldsymbol{\Phi}_{\Omega_2}(0)$	|difference|
Φ_1	$0.4521 - 0.0448\,\mathrm{i}$	$0.4521 - 0.0449\,\mathrm{i}$	$3.744 \cdot 10^{-5}$
Φ_2	$-0.1873 - 0.2693\,\mathrm{i}$	$-0.1873 - 0.2693\,\mathrm{i}$	$7.971 \cdot 10^{-6}$
Φ_3	$0.0190 + 0.0203\,\mathrm{i}$	$0.0190 + 0.0203\,\mathrm{i}$	$7.730 \cdot 10^{-6}$
	$\boldsymbol{\Phi}_{\Omega_3}(\mathrm{end})$	$T^+_{\mathrm{tot}}\boldsymbol{\Phi}^{\mathrm{in}}$	
Φ_1	$0.0671 - 0.1847\,\mathrm{i}$	$0.0671 - 0.1848\,\mathrm{i}$	$2.792 \cdot 10^{-5}$
Φ_2	$-0.1926 + 0.2528\,\mathrm{i}$	$-0.1926 + 0.2528\,\mathrm{i}$	$2.812 \cdot 10^{-5}$

Table 1: Comparing the RT and DtN method. Above: Φ_1, Φ_2 and Φ_3 at the border between Ω_1 and Ω_2 calculated with the two different methods. Below: Φ_1 and Φ_2 at the end of Ω_3 calculated with the two different methods. All calculations are made for $k = 15$.

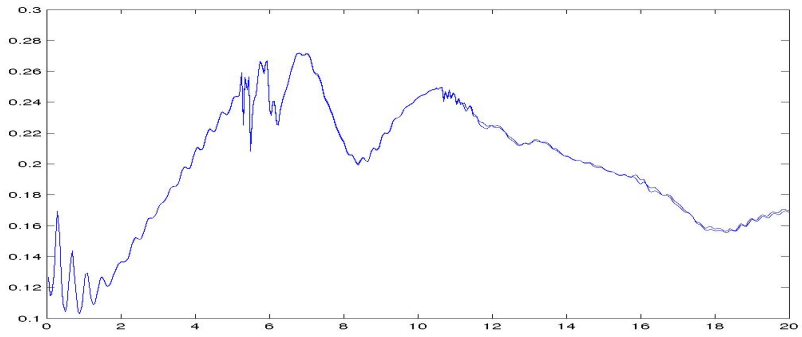

Figure 8: $|\Phi_0|$ at the end of Ω_3 calculated for $k = 0.05, 0.1, \ldots, 20$ with the Fourier methods described in the article and with the Finite Element Method.

For example, the methods in this article seem to require smooth changes in both geometry and boundary conditions to get converging Fourier series. However, the Building Block method and well-established mode-matching techniques can overcome most such problems. Furthermore, as is illustrated in [15] where an L-bend is investigated, good results can be achieved even when the conformal mapping functions contain singularities on the boundary. It is however evident that the differential equations get stiffer and that larger truncated matrices are required.

Another simplification in this article is the assumption of a Neumann boundary condition on one of the boundaries. An iterated use of the Building Block method and lengthways partitions of the waveguide can handle two-dimensional waveguides with non-hard walls on both sides.

Finally, it is possible to extend the techniques to cover three-dimensional problems, at least when variations in the geometry take place in at most two dimensions at the time. We refer to the discussion in [15].

The most time-consuming part of the calculations is the determination of the matrices A and B^2 in (18) for a large set of u-values. For every value of u, $\lambda_n(u)$ for $n = 0, \ldots, N-1$ should be found by solving equation (12) numerically. The values of α and β in eqs. (15) and (16) can be determined analytically, but for every u, N^2 numerical integrations are needed to determine the values of $\mu_{mn}(u)$ in Eq. (17). For values of u, corresponding to hard boundaries, $\lambda_n = n\pi$ and the μ coefficients can be calculated using Fast Fourier Transforms, but for values of u corresponding to boundaries with admittance, a comparatively slow numerical integration must be used for each matrix element.

However, as is seen in Figure 9, for k in the low frequency domain that we have investigated, the number of required matrix elements is modest. In the figure, the calculated values of $\left|T^+_{\text{tot}}(0,0)\right|$ and $\left|T^+_{\text{tot}}(1,0)\right|$, when using

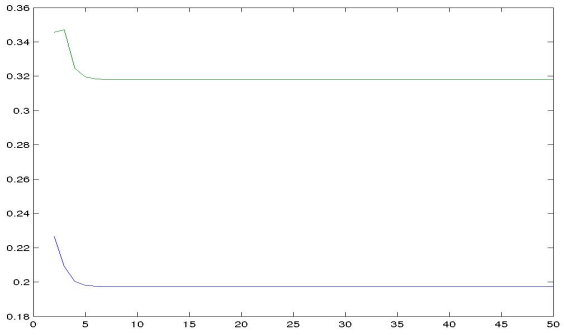

Figure 9: $\left|T^{\mathrm{tot}}(0,0)\right|$ and $\left|T^{\mathrm{tot}}(1,0)\right|$ for $k = 15$ calculated using matrices of size $N \times N$ with $N = 2 \ldots 50$.

matrix sizes from 2×2 up to 50×50, are plotted. The results are stable to three significant figures already for 7×7 matrices.

As a reference and comparison, the problem in the example has been solved using commercial software for the finite element method (FEM). As was seen in Figure 8, the correspondence between a FEM solution and the Fourier methods solution is good, with a small tendency to growing discrepancy with growing k. This is not surprising; to maintain a certain accuracy when k increases, both methods require enhanced numerical work. In FEM, a finer mesh is needed, for details see for example [8], while the Fourier methods require larger matrices.

For wave scattering problems, the Fourier methods described in this article are applicable for the low frequency domain. It is beyond the scope of this paper to develop more precise bounds for this domain. We can only conclude that the combination of semi-analytic techniques evolved here is a well working alternative to different FEM-based numerical methods.

References

[1] Anders Andersson. Schwarz–Christoffel mappings for nonpolygonal regions. *SIAM J. Sci. Comput.*, 31(1):94–111, 2008.

[2] Anders Andersson. Modified Schwarz-Christoffel mappings using approximate curve factors. *J. Comp. Appl. Math.*, 233(4):1117 – 1127, 2009.

[3] Anders Andersson and Börje Nilsson. Electro-magnetic scattering in variously shaped waveguides with an impedance condition. In *AIP Conference Proceedings: 3rd Conference on Mathematical Modeling of Wave Phenomena*, volume 1106, pages 36–45. AIP, 2009.

[4] F. Bauer. On the completeness of biorthogonal systems. *Mich. Math. J.*, 11(4):379–383, 1964.

[5] F. Bauer. Corrections to "On the completeness of biorthogonal systems". *Mich. Math. J.*, 12(1):127–128, 1965.

[6] L. Fishman, A. K. Gautesen, and Z. Sun. An exact, well-posed, one-way reformulation of the Helmholtz equation with application to direct and inverse wave propagation modeling. In *New Perspectives on Problems in Classical and Quantum Physics: A Festschrift in Honor of Herbert Überall*, pages 75–97. CRC Press, 1998.

[7] R. Glav. The transfer matrix for a dissipative silencer of arbitrary cross-section. *J. Sound. Vib.*, 236(4):575–594, 2000.

[8] Frank Ihlenburg. *Finite element analysis of acoustic scattering*, volume 132 of *Applied Mathematical Sciences*. Springer-Verlag, New York, 1998.

[9] D. S. Jones. *Acoustic and electromagnetic waves*. Oxford University press, Oxford, 1986.

[10] D. M. Kerns. Basis of the application of network equations to waveguide problems. *J. Res. natn. Bur. Stand.*, 42:515–540, 1949.

[11] Ren-Cang Li and William Kahan. A family of anadromic numerical methods for matrix Riccati differential equations. *Math. Comp.*, 81(277):233–265, 2012.

[12] J. Locker. *Spectral Theory of Non–Self–Adjoint Two–Point Differential Operators*, volume 73 of *Mathematical Surveys and Monographs*. American Mathematical Society, Providence, Rhode Island, 2000.

[13] Ya Yan Lu. Exact one-way methods for acoustic waveguides. *Math. Comput. Simulation*, 50(5-6):377–391, 1999.

[14] B. Nilsson and O. Brander. The propagation of sound in cylindrical ducts with mean flow and bulk reacting lining - IV. Several interacting discontinuities. *IMA J. Appl. Math*, 27:263–289, 1981.

[15] Börje Nilsson. Acoustic transmission in curved ducts with various cross-sections. *Proc. R. Soc. Lond. A*, 458:1555–1574, 2002.

[16] R. Young. On complete biorthogonal systems. *Proc. Am. Math. Soc.*, 83(3):537–540, 1981.